Regular Paper

Thylakoid Localized Type 2 NAD(P)H Dehydrogenase NdbA Optimizes Light-Activated Heterotrophic Growth of *Synechocystis* sp. PCC 6803

Tuomas Huokko[1,2], Dorota Muth-Pawlak [iD][1,2], and Eva-Mari Aro[1,*]

[1]Laboratory of Molecular Plant Biology, Department of Biochemistry, University of Turku, Tykistökatu 6 A, Turku FI-20014, Finland
[2]These authors contributed equally to this work.
*Corresponding author: E-mail, evaaro@utu.fi; Fax, +358 (0)29 450 5040.
(Received November 2, 2018; Accepted February 26, 2019)

NdbA, one of the three type 2 NAD(P)H dehydrogenases (NDH-2) in *Synechocystis* sp. PCC 6803 (hereafter *Synechocystis*) was here localized to the thylakoid membrane (TM), unique for the three NDH-2s, and investigated with respect to photosynthetic and cellular redox metabolism. For this purpose, a deletion mutant ($\triangle ndbA$) and a complementation strain overexpressing NdbA ($\triangle ndbA::ndbA$) were constructed. It is demonstrated that NdbA is expressed at very low level in the wild-type (WT) *Synechocystis* under photoautotrophic (PA) growth whilst substantially higher expression occurs under light-activated heterotrophic growth (LAHG). The absence of NdbA resulted in non-optimal growth of *Synechocystis* under LAHG and concomitantly enhanced the expression of photoprotection-related flavodiiron proteins and carbon acquisition-related proteins as well as various transporters, but downregulated a few iron homeostasis-related proteins. NdbA overexpression, on the other hand, promoted photosynthetic pigmentation and functionality of photosystem I under LAHG conditions while distinct photoprotective and carbon concentrating proteins were downregulated. NdbA overexpression also exerted an effect on the expression of many signaling and gene regulation proteins. It is concluded that the amount and function of NdbA in the TM has a capacity to modulate the redox signaling of gene expression, but apparently has a major physiological role in maintaining iron homeostasis under LAHG conditions. LC-MS/MS data are available via ProteomeXchange with identifier PXD011671.

Keywords: Electron transport • Light-activated heterotrophic growth • NDH-2 dehydrogenase • Photosynthesis • Proteomics • *Synechocystis* • Thylakoid.

Introduction

Both the photosynthetic and respiratory electron transfer chains reside in the thylakoid membrane (TM) of oxygen evolving photosynthetic cyanobacteria, thus differing from the TMs of photosynthetic eukaryotic organisms (for a review, see Vermaas 2001, Mullineaux 2014). Cyanobacteria additionally have a simpler respiratory electron transfer chain in the plasma membrane (PM). In respiration, ATP is produced by making use of the proton-motive force established when electrons derived from organic compounds are transferred via the electron transfer chain to terminal oxidases which donate electrons to molecular oxygen forming H_2O. One of the most important groups of proteins participating in bacterial-type respiration comprise the two types of pyridine nucleotide dehydrogenases, type 1 and type 2 NAD(P)H dehydrogenases (NDH-1 and NDH-2, respectively) (for a review, see Melo et al. 2004, Peltier et al. 2016). NDH-1 enzymes are complexes consisting of several subunits, and they pump protons across the membrane similar to the mitochondrial complex I (Strand et al. 2017). In cyanobacteria, NDH-1 complexes are localized in TM and are involved, besides respiration, in cyclic electron transfer and in C_i uptake (for a review, see Battchikova et al. 2011, Peltier et al. 2016). In contrast to NDH-1, NDH-2s are single polypeptides with molecular masses around 50 kDa and lack the ability for proton translocation across the membrane (Yagi 1991). NDH-2s typically have two GXGXXG motifs within the β-sheet–α-helix–β-sheet domains (Rossman fold) binding NAD(P)H and FAD or FMN (Wierenga et al. 1986). Nevertheless, the exact mechanism of NADH: quinone oxidoreduction by NDH-2s remains still unclear, yet hypothesis concerning the mechanism was recently proposed (Marreiros et al. 2017).

Even though all sequenced cyanobacterial species encode at least one NDH-2 enzyme in their genomes (Marreiros et al. 2016), the exact functional roles and locations of NDH-2s still remain elusive. When NDH-2 is the only enzyme capable of NADH oxidation in an organism, it is straightforward to address the main function for NDH-2 in respiratory chain-linked NADH turnover and eventual creation of the H^+-gradient for ATP production (for a review, see Melo et al. 2004). Nevertheless, *Synechocystis* sp. PCC 6803 (hereafter *Synechocystis*) has several NADH oxidizing enzymes and research on their NDH-2s has rather pointed to a regulatory role than to the function in providing energy for metabolic needs (Howitt et al. 1999). The genome of *Synechocystis* possesses three genes encoding NDH-2s, *ndbA* (*slr0851*), *ndbB* (*slr1743*) and *ndbC* (*sll1484*) (Kaneko et al. 1996, Howitt et al. 1999). Recently, it was shown that NdbB is involved in vitamin K_1 biosynthesis (Fatihi et al. 2015) and NdbC was assigned to have a significant role in regulation of carbon allocation between storage and the

biosynthesis pathways, being essential under heterotrophic growth conditions (Huokko et al. 2017).

To elucidate the role of NdbA, a deletion mutant and a corresponding complementation strain, that eventually over-expressed NdbA, were constructed followed by a thorough physiological and biochemical characterization of the strains, including the proteomic analyses. Here, we demonstrate that NdbA is located in the TM and its absence or overproduction does not exert any major effect on growth, photosynthetic capacity or expression of other proteins in respective strains under photoautotrophic (PA) conditions. Instead, the growth under light-activated heterotrophic growth (LAHG) conditions resulted in elevated level of NdbA in the TM of WT *Synechocystis* while the NdbA deletion strain demonstrated a growth retardation phenotype. NdbA overproduction, however, did not further enhance growth but maintained high photosynthetic pigmentation and oxidation capacity of photo-system I (PSI). Based on proteome analysis, the amount and function of NdbA in the TM has a capacity to modulate the redox signaling of gene expression, but apparently has a major physiological role in maintaining iron homeostasis under LAHG conditions.

Results

Construction of the *ndbA* mutant strains and the Δ*ndbA*::*ndbA* complementation strain

To evaluate the role of NdbA in *Synechocystis* redox metabolism, we constructed deletion Δ*ndbA* and complementation for *ndbA* deletion Δ*ndbA*::*ndbA* strain. The segregation of Δ*ndbA* strain was confirmed by PCR analysis (Supplementary Fig. S1A), and the absence of NdbA protein was shown by the Western blot analysis using isolated total proteins and specific antibody raised against NdbA (Agrisera) (**Fig. 1A**). The complementation strain for *ndbA* deletion, Δ*ndbA*::*ndbA*, was obtained by trans-forming the Δ*ndbA* mutant with a functional *ndbA* gene under a *psbAII* promoter (for details see Materials and Methods section). The correct insertion and the segregation were verified by PCR analysis (Supplementary Fig. S1B). The expression level of NdbA protein in the Δ*ndbA*::*ndbA* strain, immunodetected from the total protein extract using α-NdbA, was remarkably
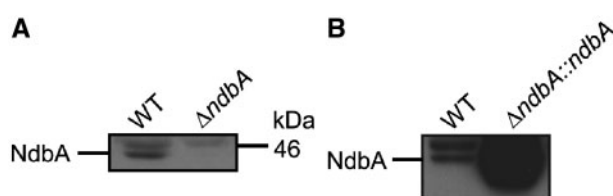

Fig. 1 Western blot analysis with α-NdbA. (A) Total proteins from WT and Δ*ndbA* immunoblotted with NdbA-antibody; (B) total pro-teins from WT and Δ*ndbA*::*ndbA* immunoblotted with NdbA-anti-body. The lower band, missing from Δ*ndbA* in (A) represents the NdbA protein. Cells were grown under photoautotrophic conditions for 4 days, 30 μg of isolated total proteins was loaded in each lane.

higher than in WT under both PA and LAHG conditions (**Figs. 1B, 3B**).

Growth of the Δ*ndbA* mutant and the Δ*ndbA*::*ndbA* strain under PA, photomixotrophic and LAHG conditions

The growth of the WT, Δ*ndbA* and Δ*ndbA*::*ndbA* strains was monitored for several days under PA, photomixotrophic (MIXO) and LAHG conditions. No differences in growth rates were observed based on optical density (OD_{750}) between the cells grown under either PA or MIXO conditions (**Fig. 2A, B**). In contrast, under LAHG conditions, after 2 d the Δ*ndbA* growth decreased compared to WT, but the Δ*ndbA*::*ndbA* strain con-tinued to grow similar to WT (**Fig. 2C**). Based on these obser-vations, we chose the PA and LAHG conditions to further characterize the function of NdbA protein in *Synechocystis* metabolism.

Cellular localization of NdbA and expression under PA and LAHG conditions

To specify the localization of NdbA in *Synechocystis* cell, the Western blotting with NdbA-specific antibody was applied to the protein fractions of TM and PM as well as to the soluble fraction (SF). Immunoblotting with α-NdbA clearly indicated that NdbA resided in TM while no signal was detected from the PM and SF (**Fig. 3A**). In addition, the expression level of NdbA under PA and LAHG conditions was estimated from the total protein extract, based on Western blot analysis. In WT, the amount of NdbA under LAHG conditions was clearly higher than under PA conditions while the complementation Δ*ndbA*::*ndbA* strain showed distinct overexpression of NdbA under both the PA and LAHG conditions, yet with higher ac-cumulation of NdbA under PA condition (**Fig. 3B**). This is in accordance with the use of light sensitive *psbAII* promoter for construction of the complementation strain but it is worth noting that clear activation of the promoter also occurred under LAHG conditions despite only short daily illumination periods (**Fig. 3B**).

Ultrastructure of the Δ*ndbA* mutant and the Δ*ndbA*::*ndbA* strain under LAHG conditions

The ultrastructure of WT, Δ*ndbA* and Δ*ndbA*::*ndbA* cells grown under LAHG condition was investigated with the trans-mission electron microscopy (TEM) (**Fig. 4**). Under these con-ditions in WT (**Fig. 4A**) and in the Δ*ndbA* mutant (**Fig. 4B**) similar amount of thylakoids were present but the Δ*ndbA*::*ndbA* strain (**Fig. 4C**) retained higher TM content. However, there was no significant difference in the cell size between the studied strains.

Pigment phenotype and the room temperature whole cell absorption spectra under LAHG conditions

After 4 d of growth under LAHG conditions the color pheno-types of WT culture, the Δ*ndbA* culture and the Δ*ndbA*::*ndbA* culture were different from each other: Δ*ndbA* was paler green
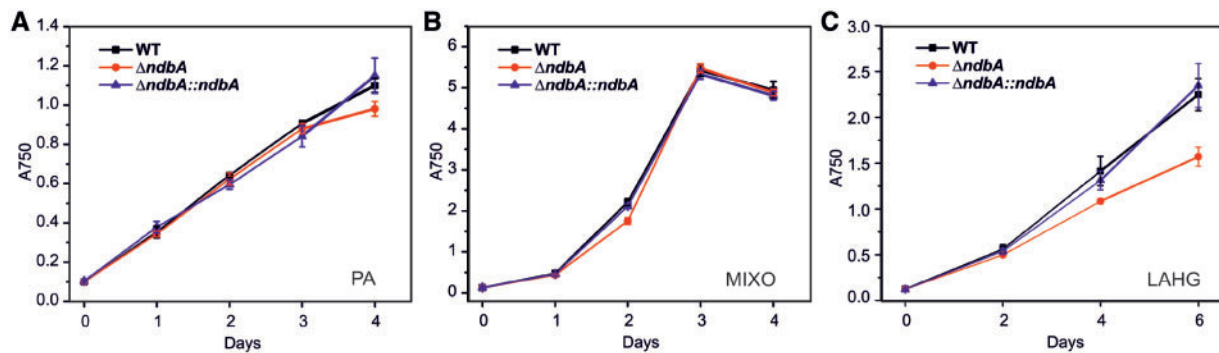
Fig. 2 The growth of WT (black squares), $\Delta ndbA$ (red circles) and $\Delta ndbA::ndbA$ (blue triangles) under (A) photoautotrophic (PA) conditions with continuous illumination of 50 µmol photons m^{-2} s^{-1}; (B) photomixotrophic (MIXO) conditions (continuous illumination of 50 µmol photons m^{-2} s^{-1}, 10 mM glucose) and (C) light-activated heterotrophic growth (LAHG) conditions (50 µmol photons m^{-2} s^{-1} light for 10 min once in 24 h, 10 mM glucose). At the beginning of experiments, the cells were inoculated at OD_{750} = 0.1. Values are means ±SD. n = 3.

Fig. 3 Expression of NdbA in Synechocystis with Western blot analysis with α-NdbA. (A) the thylakoid membrane (TM), the plasma membrane (PM) and the soluble fractions (SF) of WT cells immunoblotted with α-NdbA, α-NdbC and α-APC. All the cells for protein isolation were grown under photoautotrophic (PA) conditions and 10–25 µg of total proteins were loaded in each lane. (B) WT, $\Delta ndbA$ and $\Delta ndbA::ndbA$ strains grown under photoautotrophic (PA) and light-activated heterotrophic growth (LAHG) conditions. Cells were collected after 4 d. Thirty micrograms (100%) of total proteins were loaded per lane immunoblotted with α-NdbA. In total is not necessary 10–50% refers to fraction of total protein amount (30 µg) loaded.

compared to WT whereas the clearly greenest phenotype was expressed by $\Delta ndbA::ndbA$ (**Fig. 5A**). To further analyze the difference in pigment composition, the room temperature whole cell absorption spectra were recorded from strains grown for 4 d under LAHG conditions. Before measurements, the samples were normalized to the same OD_{750}. No differences were observed in the spectra between $\Delta ndbA$ and WT (**Fig. 5B**), whereas the spectra of the $\Delta ndbA::ndbA$ strain demonstrated substantially higher peaks of chlorophyll a (Chl; peaks at 440 nm and 680 nm), phycobilins (peak at 626 nm) and carotenoids (peak at 480–490 nm) compared to WT and $\Delta ndbA$.

Differential protein expression in $\Delta ndbA$ and $\Delta ndbA::ndbA$ under PA and LAHG conditions

The consequences of the cellular amount of the NdbA protein on global protein expression in Synechocystis were investigated by label free mass spectrometry (MS) data dependent acquisition (DDA). The whole cell protein extracts from $\Delta ndbA$, $\Delta ndbA::ndbA$ and WT strains grown under PA and LAHG conditions were digested and analyzed, in untargeted manner, by liquid chromatography coupled to tandem mass spectrometry system (LC-MS/MS). The samples were injected in biological

quadruplicates. In 12 independent mass spectrometry runs performed for PA and LAHG condition, we identified and then quantified (with at least 2 peptides) 2085 and 2136 proteins under PA and LAHG condition respectively (Supplementary Tables S1, S2). The results of relative quantification were further filtered with statistical significance cut-off set to P-value ≤0.05 and the fold change (FC) threshold of the practical significance set to $-1.4 \leq$ FC and FC ≥ 1.4.

Under PA conditions the deletion of NdbA resulted in 15 upregulated and downregulated proteins (Supplementary Table S3) whereas the overexpression of NdbA resulted in upregulation of 9 and in downregulation of 16 proteins compared to WT (Supplementary Table S4). With the same significance and practical thresholds, the deletion of NdbA under LAHG conditions resulted in upregulation of 44 and downregulation of 19 proteins (Supplementary Table S5) compared to WT, whereas the overexpression of NdbA resulted in upregulation of 223 and downregulation of 102 proteins compared to WT (Supplementary Table S6).

We first used the proteomics data to confirm the content of the NdbA protein in different strains under the PA and LAHG growth conditions. The NdbA protein was identified in WT grown under LAHG conditions and in $\Delta ndbA::ndbA$ strain grown under PA and LAHG conditions. This is the first time
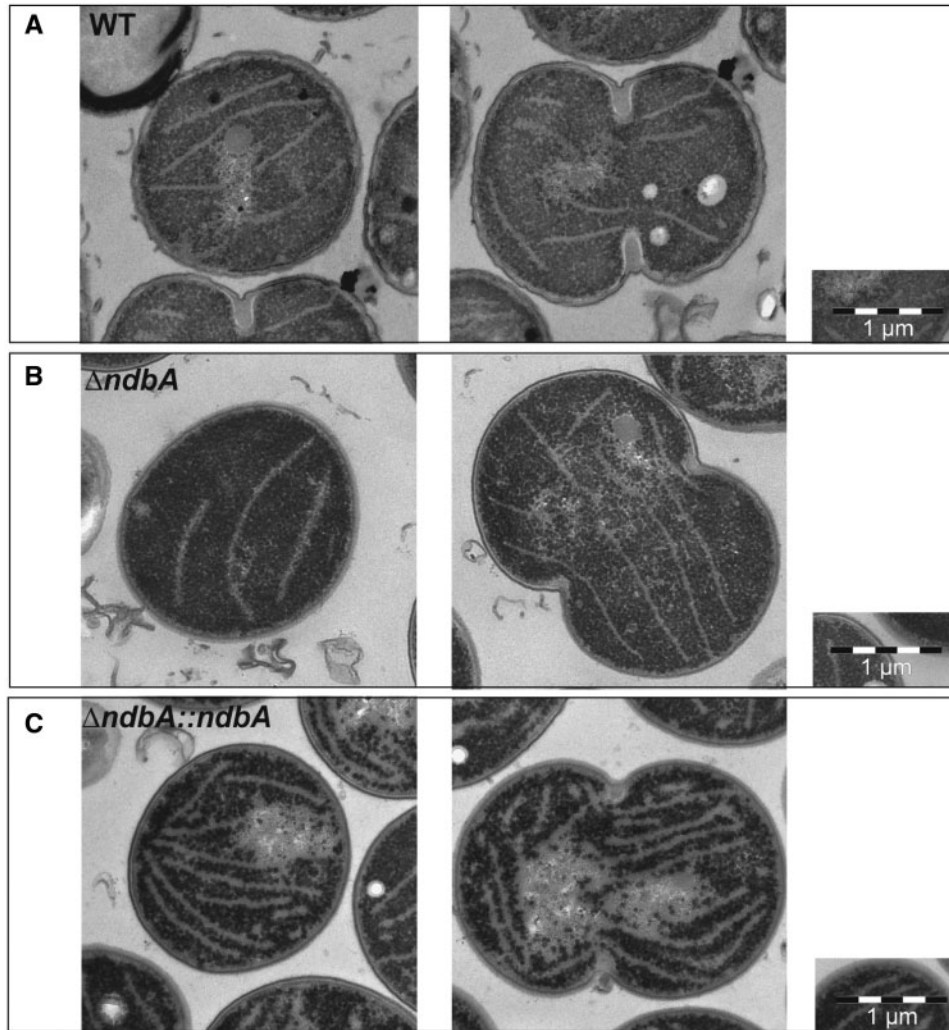
Fig. 4 Transmission electron microscope (TEM) images of WT (A), Δ*ndbA* (B) and Δ*ndbA::ndbA* (C) cells grown under light-activated heterotrophic growth (LAHG) conditions. Cells were collected after 4 days. Figures are representatives of 100 cells photographed for every line.
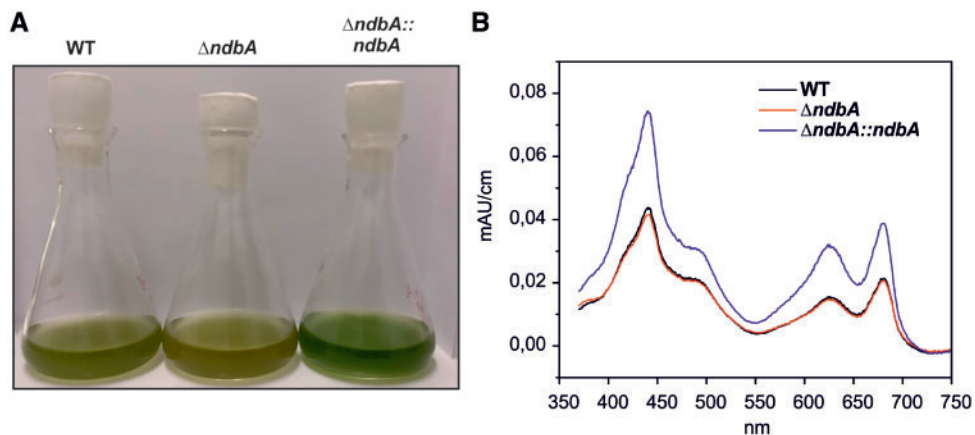
Fig. 5 The color difference between WT, Δ*ndbA* and Δ*ndbA::ndbA* grown under light-activated heterotrophic growth (LAHG) conditions. (A) The color phenotype of WT, Δ*ndbA* and Δ*ndbA::ndbA* cultures grown under LAHG conditions for 4 days. (B) The whole cell absorption spectra at room temperature from WT (black line), Δ*ndbA* (red line) and Δ*ndbA::ndbA* (blue line) grown under LAHG conditions. OD_{750} was adjusted to 0.3 before recording the absorption spectra. Each curve is an average from four biological repetitions.

Fig. 6 NdbA abundance based on DDA in WT (black bars), Δ*ndbA* (grey bars) and Δ*ndbA::ndbA* (white bars) under photoautotrophic (PA) conditions and under light-activated heterotrophic growth (LAHG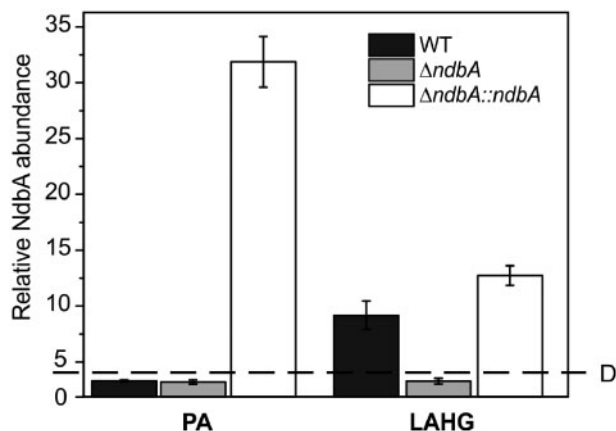) conditions. Cells were collected after 4 days. Dashed line indicates detection level. Values are means ± SD, $n = 3$–4.

when NdbA is detected in WT by MS from unfractionated cell lysate. The NdbA abundance in WT grown under PA conditions remained under the detection level of mass spectrometer while it was distinct under LAHG conditions. At the same time, the Δ*ndbA::ndbA* overexpression strain showed elevated abundance of NdbA under PA, which also remained higher than that in WT under LAHG conditions (**Fig. 6**) in accordance to immunodetection results (**Fig. 3B**).

The global proteomes of the three strains grown under PA conditions demonstrated only minor differences. The inducible ABC-type HCO_3^- transporter BCT1 (Omata et al. 1999), indicated by CmpB and CmpC, was found to be downregulated in both Δ*ndbA* and Δ*ndbA::ndbA* compared to WT (Supplementary Tables S3, S4). In addition, the amounts of Hik36 and Hik43 were higher in both mutant strains compared to WT. Transporters functioning in K uptake (KdpA, KdpB and KdpC) were strongly upregulated in Δ*ndbA* compared to WT, but this was not observed in the Δ*ndbA::ndbA* strain. The rest of proteins remained below the statistical and significance threshold.

WT, ΔndbA and ΔndbA::ndbA cells grown under LAHG conditions demonstrated distinct variations in protein expression, covering diverse functional groups as photosynthesis and respiration, regulatory functions, carbon assimilation and nitrogen metabolism as well as cellular transport. Photosynthesis and respiration related proteins were the most affected in Δ*ndbA::ndbA* strain as components of photosystem II (PSII), including PsbA (D1), PsbB (CP47), PsbD (D2), PsbC (CP43), PsbO, PsbV, PsbE, PsbQ and Psb32, were at elevated level as compared to WT (**Table 1**). In addition, the proteins involved in PSII assembly as sll0933, slr0147 and slr0151 were also upregulated in overexpression line. The Cyt *b₆f* complex proteins PetA, B and C were upregulated only in the Δ*ndbA::ndbA* strain compared to WT. In addition, the amounts of several soluble electron carriers, including Cyt c_6 and several Ferredoxins (Feds 2, 3, 5 and 7) were elevated in the Δ*ndbA::ndbA* strain compared to WT.

As to the regulatory proteins of thylakoid electron transfer, the amounts of the flavodiiron proteins Flv2 and Flv4, involved in the protection of PSII (Zhang et al. 2009, Zhang et al. 2012, Bersanini et al. 2014), were distinctively elevated in Δ*ndbA* under LAHG conditions (**Table 1**). Interestingly, these same proteins were downregulated in Δ*ndbA::ndbA* as compared to WT (**Table 1**) together with downregulation of the orange carotenoid protein (OCP) (**Table 1**), which performs non-photochemical quenching (NPQ) in several cyanobacterial species (Wilson et al. 2006, Wilson et al. 2007, Boulay et al. 2010) (for a review, see Kirilovsky and Kerfeld 2013). Conversely, the fluorescence recovery protein (FRP) required for deactivation of OCP during NPQ was downregulated in Δ*ndbA* but upregulated in Δ*ndbA::ndbA* (**Table 1**). The expression of several phycobilisome (PBS)-related proteins (CpcD, CpcA, ApcF, CpcG, CpcC1 and Cpc2) was elevated in the Δ*ndbA::ndbA* strain compared to WT (**Table 1**). The three enzymes involved in Chl and bilin biosynthesis as HemF, HemH, Ho1 and ChlA₁ were upregulated. Similarly, the amounts of proteins involved in later steps of Chl biosynthesis, including ChlB, ChlN and ChlL were higher in Δ*ndbA::ndbA* compared to WT, whereas in ChlG-amount was lower in both Δ*ndbA::ndbA* and Δ*ndbA* strains compared to WT. Interestingly, also geranylgeranyl reductase (ChlP), responsible for reduction of geranylgeranyl chain in Chl biosynthesis and free diphosphate in tocopherol and phylloquinone derivatives biosynthesis, was upregulated (**Table 1**). In addition, carotenoids biosynthesis pathway enzymes Pys (slr1255) and CrtU showed upregulation, while astaxanthin biosynthesis branch represented by CrtO was downregulated.

In addition to photosynthetic components, the absence or overproduction of the NdbA protein in the TM under LAHG conditions exerted an effect on the expression of several proteins involved in C_i assimilation. Both inducible HCO_3^- uptake systems, the ABC-type bicarbonate transporter BCT1 (CmpB, C) (Omata et al. 1999) and the Na^+ dependent bicarbonate transporter SbtA (Shibata et al. 2002), were upregulated in the Δ*ndbA* mutant compared to WT (**Table 1**). Also the amount of low-CO_2-inducible, high-affinity CO_2 uptake complex NDH-1_3 (for a review, see Battchikova et al. 2011, Peltier et al. 2016) was higher in the Δ*ndbA* mutant compared to WT, indicated by upregulation of the NDH-1_3 –specific subunits CupA and CupS (**Table 1**). The Δ*ndbA::ndbA* strain behaved differently. Proteins related to the carbon concentration mechanisms (CCM) including BCT1 (indicated by CmpA, CmpB and CmpC) and SbtA, SbtB as well as the NDH-1_3 complex (represented by NdhF3 and CupA) were downregulated in Δ*ndbA::ndbA* as compared to WT (**Table 1**).

Under LAHG, the amount of several proteins involved in N assimilation were elevated in the Δ*ndbA::ndbA* strain compared to WT. These included NrtA and NrtD, which are subunits of the NRT transporter. In addition, nitrogen reductase proteins, like ferredoxin-nitrate reductase NarB and NarM, were upregulated (**Table 1**). Further, the amounts of transporters that function in P_i uptake (PstS1, PstS2 and SphX) as well as in K uptake (KdpA, KdpB and KdpC) were higher in both mutant strains compared to WT. The CopMRS and CopBAC systems responsible for copper homeostasis in the cell were downregulated in the Δ*ndbA::ndbA* strain while SynAtx1, the

PCP
PLANT & CELL PHYSIOLOGY

Table 1 Differential protein expression in the Δ*ndbA* mutant versus WT and in the Δ*ndbA::ndbA* strain versus WT grown under light-activated heterotrophic growth (LAHG) conditions and investigated by data dependent acquisition (DDA)

Function	Protein		FC ΔndbA/WT LAHG	ANOVA (P-value)	FC ΔndbA::ndbA/WT LAHG	ANOVA (P-value)
PSII	slr1311	PsbA2 (D1)	1.3	1.98E−02	**1.5**	2.54E−03
	sll0849	PsbD (D2)	**1.5**	7.72E−03	**2.0**	1.35E−03
	sll0851	PsbC (CP43)	1.1	1.16E−01	**1.5**	3.84E−03
	ssr3451	PsbE	1.3	1.60E−03	**2.1**	2.94E−06
	sll0258	PsbV	1.3	3.57E−03	**1.8**	2.15E−04
	sll0427	PsbO	1.2	9.41E−02	**1.6**	2.71E−04
	sll1638	PsbQ	1.2	4.94E−02	**1.4**	3.35E−03
	sll1390	Psb32	1.1	4.44E−01	**1.4**	1.27E−04
	sll0933	PSII assembly factor	−1.1	4.35E−01	**1.4**	3.04E−02
	slr0147	PSII assembly factor	1.1	4.57E−01	**1.4**	2.39E−03
	slr0151	PSII assembly factor	−1.0	7.03E−01	**1.4**	8.84E−04
Cyt b₆f	sll1317	PetA	1.1	1.25E−01	**1.5**	8.65E−04
	slr0342	PetB	1.1	1.11E−01	**1.5**	1.96E−03
	sll1316	PetC	1.0	6.33E−01	**1.5**	2.54E−03
Soluble electron carriers	sll1796	Cytc₆, PetJ	**−1.8**	1.24E−01	**2.8**	1.86E−02
	sll1382	Fed2	−1.1	1.36E−01	**2.2**	6.90E−04
	slr1828	Fed3	−1.1	3.99E−01	**1.7**	3.22E−02
	ssl2559	Fed5	1.2	1.53E−01	**1.4**	2.07E−02
	sll0662	Fed7	1.1	5.35E−01	**1.6**	1.85E−02
Photoprotection of PSII	sll0217	Flv4	**2.0**	2.70E−02	**−1.8**	4.92E−02
	sll0219	Flv2	**2.1**	1.51E−02	**−1.5**	2.56E−02
	slr1963	Ocp	−1.0	9.52E−01	**−1.5**	2.28E−06
	slr1964	Frp	−1.3	1.57E−02	**1.5**	1.29E−02
Phycobilosomes	slr1459	ApcF	1.0	7.20E−01	**1.4**	2.69E−04
	sll1580	CpcC1	1.1	1.21E−01	**1.4**	2.26E−03
	sll1471	CpcG	1.9	2.63E−04	**2.1**	6.15E−06
	ssl3093	CpcD	1.1	2.52E−01	**1.4**	3.98E−04
	sll1578	CpcA	1.1	4.12E−01	**1.4**	2.42E−02
	sll1579	CpcC2	1.2	4.25E−03	**1.6**	9.35E−05
Chlorophyll and bilin biosynthesis	sll1185	HemF	−1.0	7.31E−01	**1.7**	1.47E−05
	slr0839	HemH	1.1	2.54E−01	**1.6**	7.56E−04
	sll1184	Ho1	−1.1	5.38E−01	**2.1**	1.23E−04
	sll1214	ChlAI	−1.1	1.06E−02	**1.7**	8.28E−05
	slr0056	ChlG	**−1.6**	2.30E−02	**−1.9**	6.43E−03
	slr0749	ChlL	−1.2	3.51E−01	**1.8**	2.21E−02
	slr0750	ChlN	−1.2	2.58E−02	**1.8**	1.94E−05
	slr0772	ChlB	−1.1	1.19E−01	**2.7**	8.09E−06
	sll1091	ChlP	−1.2	1.14E−02	**2.0**	1.06E−04
Carotenoids biosynthesis	slr1255	Pys, CrtB	−1.2	7.01E−02	**1.6**	2.86E−03
	slr0088	CrtO	1.0	9.24E−01	**−1.6**	2.00E−03
	sll0254	CruE	**−1.4**	3.48E−02	**1.9**	1.40E−04
Carbon concentratin mechanism	slr1512	SbtA	1.3	1.88E−02	**−2.0**	7.44E−04
	slr1513	SbtB	1.1	1.70E−01	**−1.6**	1.50E−03
	sll1734	CupA	1.3	2.91E−02	**−1.7**	1.19E−03
	sll1732	NdhF3	**1.9**	7.16E−02	**−3.4**	1.22E−02
	slr0040	CmpA	**3.1**	1.58E−01	**−4.1**	4.58E−02
	slr0041	CmpB	**3.4**	2.67E−02	**−5.9**	5.85E−03
	slr0043	CmpC	**3.0**	1.75E−02	**−2.9**	7.62E−03
Nitrogen assimilation	sll1451	NrtB	1.0	9.62E−01	**1.5**	9.57E−04
	sll1452	NrtC	−1.2	1.54E−02	**1.4**	3.86E−05
	sll1453	NrtD	−1.2	5.70E−02	**1.6**	5.48E−04
	sll1454	NarB	1.5	5.08E−01	**1.8**	7.34E−04
	sll1455	NarM	1.1	6.45E−01	**1.4**	8.17E−03
Pᵢ uptake	sll0679	SphX	**2.1**	2.52E−05	**2.0**	1.84E−01
	sll0680	PstS1	**1.7**	2.69E−03	1.4	4.67E−01
	slr1247	PstS2	**4.5**	1.08E−04	1.7	4.80E−01
K uptake	slr1728	KdpA	**2.5**	1.24E−04	**1.6**	2.68E−03
	slr1729	KdpB	**2.2**	4.24E−06	**1.8**	7.77E−05

(continued)

Table 1 Continued

Function	Protein		FC ΔndbA/WT LAHG	ANOVA (P-value)	FC ΔndbA::ndbA/WT LAHG	ANOVA (P-value)
	slr1730	KdpC	**3.0**	8.33E−05	**2.1**	1.17E−04
Fe uptake	sll1878	FutC	**−1.8**	2.93E−02	**1.9**	1.37E−02
	sll0088	SufR	**−2.0**	8.27E−03	−1.1	5.47E−01
Cu homeosthasis	sll0788	CopM	1.0	7.11E−01	**−1.4**	4.32E−02
	slr6044	CopC	1.1	7.55E−02	**−1.4**	6.36E−03
	slr6042	CopB	1.0	9.51E−01	**−1.9**	2.08E−04
	ssr2857	SynAtx1	−1.0	2.50E−01	**1.4**	1.46E−04
	sll0790	CopS, Hik31	1.1	4.14E−01	**−1.4**	9.85E−04
Others	slr0483	CurT	1.2	2.64E−02	**1.5**	2.56E−04
	slr1931	PilA8	1.1	1.58E−01	**1.4**	3.13E−03
	sll1695	PilA2	**1.8**	1.21E−03	**1.9**	6.18E−03
	slr1929	PilA6	**1.6**	9.93E−03	**1.7**	2.93E−04
	slr1928	PilA5	1.1	6.15E−01	**1.7**	6.04E−03
	slr2015	PilA9	**−1.7**	3.27E−01	**3.8**	1.85E−02
	slr0473	Hik35	1.1	5.87E−01	**1.7**	3.51E−03
	slr0073	Hik36	**−5.4**	1.06E−06	**−3.5**	2.69E−06
	slr1285	Hik34	−1.3	2.80E−01	**−3.1**	7.01E−04
	slr0474	Rre27	1.1	5.01E−01	**1.6**	3.88E−02
	slr0081	Rre29	−1.3	2.93E−01	**2.6**	4.99E−03
	slr0312	Rre32	**−1.6**	1.19E−02	**−1.5**	3.76E−02
	sll1330	Rre37	1.0	6.65E−01	**−1.4**	7.26E−04
	sll1980	TrxA	1.0	8.45E−01	**1.7**	9.30E−04
	slr0653	SigA	−1.0	4.49E−01	**1.4**	5.55E−04
	slr0851	NdbA	**−5.2**	1.39E−04	**1.5**	2.58E−02

The practical significance of the fold change (FC) is marked with bold font when upregulated (FC ≥ 1.4) or downregulated (FC ≤ −1.4) (P-value ≤ 0.05) related to WT.

protein interacting with ATPases and ensuring copper transport to thylakoid lumen, was upregulated. TM located CurT protein also showed upregulation in the ΔndbA::ndbA strain.

The expression of several proteins involved in iron metabolism and acquisition indicated significant downregulation only in the ΔndbA mutant compared to WT (**Table 1**). These included FutC, involved in ferric iron uptake (Katoh et al. 2001) and the iron–sulfur cluster biogenesis regulator SufR (Shen et al. 2007). Furthermore, the amounts of Cyt c_6 containing a heme group as well as a CruE enclosing Rieske 2Fe-2S center involved in the biosynthesis of carotenoids (Mohamed and Vermaas 2006) were present at lower level in the ΔndbA mutant compared to WT (**Table 1**).

Several histidine kinases (Hik) demonstrated different expression in the ΔndbA::ndbA strain compared to WT under LAHG conditions. The amount of Hik35 was elevated whereas the amounts of Hik36 and Hik34 were diminished (**Table 1**). Hik36 and Hik34 were likewise downregulated in ΔndbA compared to WT. In the ΔndbA::ndbA strain, the response regulators Rre29 and Rre27 were elevated at protein level but the amounts of Rre32 and Rre37 were lower compared to WT (**Table 1**), and Rre32 was downregulated also in ΔndbA. The two regulatory proteins TrxA and SigA were upregulated in ΔndbA::ndbA compared to WT (**Table 1**).

Photosynthetic characterization of the NdbA mutants under PA and LAHG conditions

For proper comparisons, the Chl fluorescence and P700 measurements were first performed with PA-grown WT, ΔndbA and

ΔndbA::ndbA cells using a Dual-PAM fluorometer. As demonstrated in **Fig. 7**, no distinct difference was observed between the strains either in the effective PSII yield, Y(II), (**Fig. 7A**) or in the effective PSI yield, Y(I), (**Fig. 7B**) measured during illumination with actinic light (50 μmol photons m^{-2} s^{-1}). Next, the same measurements were performed with the cells grown under LAHG conditions. In the WT and in ΔndbA, the effective PSII yield, Y(II), was not detectable whereas the ΔndbA::ndbA cells showed a low but considerable Y(II) level (**Fig. 7C**). The effective PSI yield, Y(I), measurements demonstrated no clear differences between WT, ΔndbA and ΔndbA::ndbA cells under LAHG conditions (**Fig. 7D**).

Functionality of PSI was further measured from WT, ΔndbA and ΔndbA::ndbA cells by measuring the maximal amount of oxidizable P700 (P_m) when cells were grown either under PA or LAHG conditions (**Table 2**). The P_m values of the WT, ΔndbA and ΔndbA::ndbA cells did not differ significantly under PA conditions. On the contrary, the P_m value of ΔndbA was significantly lower compared to WT under LAHG conditions whereas in the ΔndbA::ndbA strain the P_m value was drastically higher compared to the two other strains studied under the same conditions.

Discussion

The three NDH-2 enzymes in Synechocystis (NdbA, NdbB and NdbC) have been postulated to have regulatory roles rather than being directly involved in bioenergetic electron transfer
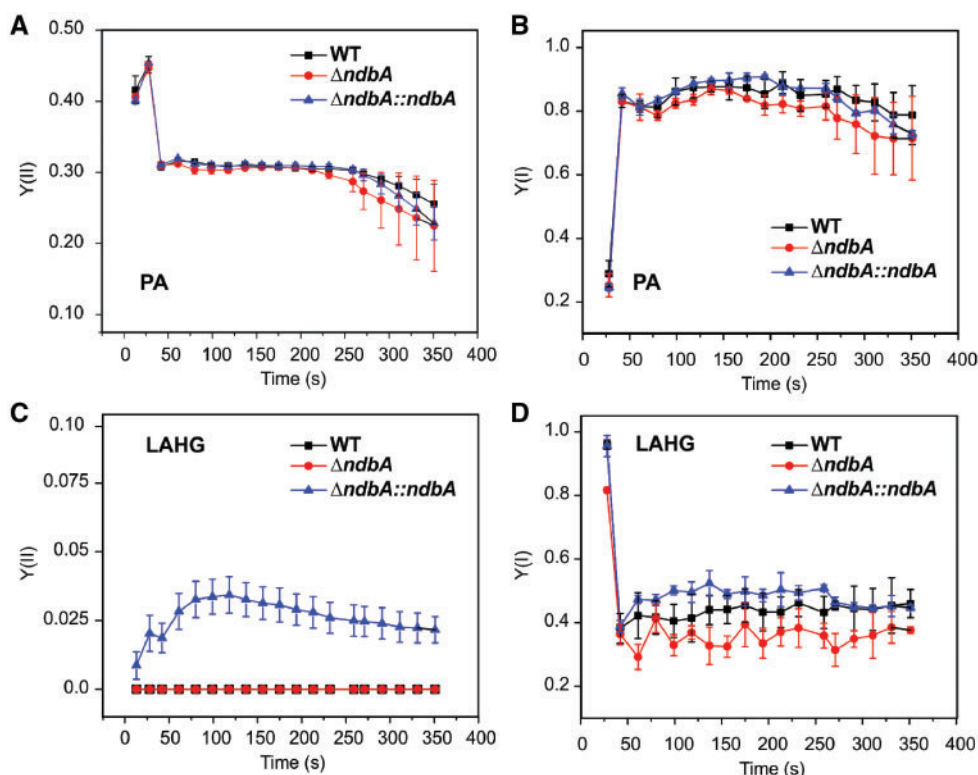
Fig. 7 Photosynthetic characterization of WT (black squares), $\Delta ndbA$ (red circles) and $\Delta ndbA::ndbA$ (blue triangles) grown under photoautotrophic (PA) and under light-activated heterotrophic growth (LAHG) conditions. (A) the effective PS II yield, Y(II), under PA; (B) the effective PSI yield, Y(I), under PA; (C) the effective PS II yield, Y(II), under LAHG; and (D) the effective PSI yield, Y(I), under LAHG. Cells were dark-acclimated for 10 min before measurements and the Chl concentration was adjusted to 15 μg ml^{-1}, and measurements were done under illumination of 50 μmol photons m^{-2} s^{-1} as actinic light. Mean ± SD. $n = 3$.

Table 2 P$_m$ values from WT, $\Delta ndbA$ and $\Delta ndbA::ndbA$ grown under photoautotrophic (PA) conditions and under light−activated heterotrophic growth (LAHG) conditions

	P$_m$
WT PA	0.08 ± 0.004
$\Delta ndbA$ PA	0.07 ± 0.005
$\Delta ndbA::ndbA$ PA	0.08 ± 0.001
WT LAHG	0.04 ± 0.003
$\Delta ndbA$ LAHG	0.03 ± 0.002*
$\Delta ndbA::ndbA$ LAHG	0.07 ± 0.003*

Values are means ± SD; $n = 3$.
*Statistically significant differences between WT and the $\Delta ndbA$ mutants ($P < 0.05$).

chains that produce ATP (Howitt et al. 1999). However, their exact roles and even the cellular localization have remained largely elusive. Quite recently, the function for NdbB in vitamin K$_1$ biosynthesis (Fatihi et al. 2015) as well as the role of NdbC in carbon allocation, its location in the PM and necessity under LAHG conditions (Huokko et al. 2017) have been demonstrated. This indicates that even though NDH-2s in *Synechocystis* catalyze the oxidation of NADH, they seem to be implicated in different metabolic pathways. In the present study, we addressed the physiological role of the third NDH-2, NdbA, which we first localized to the TM of *Synechocystis* (**Fig. 3A**), thus indicating diverse cellular compartments and reinforcing distinct functional roles for the three different NDH-2s.

NdbA is dispensable in *Synechocystis* under PA conditions

The deletion or overexpression of NdbA did not influence the growth of *Synechocystis* under PA conditions (**Fig. 2A**) which is in agreement with earlier studies by Howitt et al. (1999). In line with this, the proteome analysis of cells grown under PA conditions demonstrated only few changes caused by either the deletion or overexpression of NdbA (Supplementary Tables S3, S4). The insignificance of NdbA under photoautotrophy in *Synechocystis* is supported by the fact that only a small amount of NdbA is present in WT thylakoids since it was found only with immunodetection technique and remained below detection limit of mass spectrometer (**Figs. 3B, 6**). Likewise, the photosynthetic capacity, indicated by the effective PSII yield, Y(II), (**Fig. 7A**), the effective PSI yield, Y(I), (**Fig. 7B**) and the maximum amount of photo-oxidizable P700, P$_m$ (**Table 2**), or the pigment levels and chloroplast ultrastructure (Supplementary Fig. S2), were not altered in the mutant strains under PA conditions. These results indicated that NdbA is needed most probably under certain stress conditions or when photosynthesis is not the main way to produce energy for the growth of *Synechocystis*.

NdbA optimizes the growth of *Synechocystis* under LAHG conditions without affecting the regulation of sugar catabolism

The deletion of NdbA resulted in retarded growth of *Synechocystis* under LAHG conditions (**Fig. 2C**). Further, the growth defect of Δ*ndbA* was not caused by the inability to uptake glucose since no difference in the growth between WT and the NdbA mutant strains was observed under MIXO conditions (**Fig. 2B**). The mass spectrometry analysis (**Fig. 6**) as well immunodetection (**Fig. 3B**) data indicate that the amount of NdbA significantly increases in WT thylakoids under LAHG conditions compared to its expression under PA conditions (**Figs. 3B, 6**), being the first indication about the importance of NdbA under LAHG conditions.

The proteome analysis demonstrated no differences in the amounts of sugar catabolic proteins in the Δ*ndbA* mutant compared to WT, which may be explained by insignificant change in the expression of SigE, the general inducer of the genes functioning in sugar catabolism (Osanai et al. 2005) (**Table 1**). Thus, the growth retardation of Δ*ndbA* under LAHG conditions, as compared to WT, hardly results from problems in glucose catabolism. Indeed, upon LAHG *Synechocystis* uses glucose as a sole energy source (Plohnke et al. 2015), and the activities of sugar catabolic enzymes, glucokinase and pyruvate kinase, have been reported to be at elevated level (Knowles and Plaxton 2003). Also Gap1, an essential enzyme for glycolysis, is upregulated at the protein level under LAHG conditions (Kurian et al. 2006). Under heterotrophic conditions the oxidative pentose phosphate pathway is the most important glycolytic route (Wan et al. 2017) as it is the only source of intermediates for nucleotide biosynthesis in darkness (Kruger and Von Schaewen 2003), consuming 90% of assimilated external glucose (Yang et al. 2002). All these essential enzymes for LAHG were present at WT level in both NdbA mutants, providing evidence that NdbA is not involved in regulation of sugar catabolism in *Synechocystis*.

The apparent intactness of sugar catabolism pathways in the Δ*ndbA* mutant, opposite to that in the NdbC deletion mutant (Huokko et al. 2017), further supports the different functions of NDH-2s in *Synechocystis*. The PM-located NdbC is crucial for regulation of sugar catabolism and maintenance of growth under LAHG conditions (Huokko et al. 2017) while different mechanisms must be involved in the enhancement of LAHG growth of *Synechocystis* by the TM-localized NdbA. According to proteomics results, very few proteins were downregulated in the NdbA deletion mutant under LAHG as compared to WT (**Table 1**). These included the iron transport protein FutC, iron–sulfur cluster biogenesis regulator SufR (Shen et al. 2007) together with iron containing Cyt c_6 and CruE (**Table 1**). Such downregulation may exert a crucial effect on cell growth rate as iron is one of the most essential micronutrients for maintenance of optimal cellular metabolism and growth, for example as a building block of the iron–sulfur clusters of many regulatory and redox active proteins. This can also partially explain the reduced photosynthetic capacity of PSI in the NdbA deletion mutant under LAHG (**Table 2**).

Overexpression of NdbA maintains higher Chl and PBS content under LAHG conditions

It has been shown previously that the growth of *Synechocystis* under LAHG conditions results in significantly lower amount of Chl (Barthel et al. 2013) and pigment-binding proteins (Plohnke et al. 2015) than growth under PA conditions. After 4 d of growth under LAHG conditions, Δ*ndbA* demonstrated even paler green phenotype than WT whereas Δ*ndbA::ndbA* remained considerably greener than WT (**Fig. 5A**). Closer inspection of the absorption spectra revealed that the color difference between WT and Δ*ndbA* cultures (**Fig. 5A, B**) was caused by lower OD$_{750}$ in Δ*ndbA*. On the contrary, overexpression of NdbA in Δ*ndbA::ndbA* resulted in higher Chl, phycobilin and carotenoid content (**Fig. 5B**) as well as a higher amount of proteins involved in PBS formation and in Chl and carotenoid biosynthesis compared to WT (**Table 1**). Of the enzymes related to Chl biosynthesis, ChlA$_I$, ChlB, ChlL and ChlN were the most upregulated ones at protein level in the Δ*ndbA::ndbA* strain compared to WT under LAHG conditions (**Table 1**). These proteins (ChlB, ChlL and ChlN) form the light-independent protochlorophyllide reductase (DPOR) which catalyzes the conversion of photochlorophyllide to chlorophyllide, and this reaction is the major regulatory step of the light-independent Chl synthesis (LICS) pathway (Fujita 1996, Kada et al. 2003). Upregulation of the iron transporter FutC in the NdbA overexpression strain Δ*ndbA::ndbA* (**Table 1**) is possibly related to their enhanced biosynthesis of Chl.

It was recently demonstrated that LICS is necessary for the adequate Chl accumulation when *Synechocystis* cells are grown under light-/dark-rhythm and its importance was shown to increase when glucose was added to the growth medium (Fang et al. 2017). It is thus clear that the excess of NdbA maintains pigment biosynthesis in *Synechocystis* cells, especially by stimulating the LICS pathway. The downregulation of Chl synthase ChlG may be considered as the protective mechanism against too high accumulation of Chl, which becomes harmful for the cell if not bound to the protein complexes. The simultaneous upregulation of geranylgeranyl reductase ChlP suggests increased synthesis of tocopherol and phylloquinone derivatives that protect the cell against harmful activity of ROS (Latifi et al. 2009, Shpilyov et al. 2013). At the same time, two other pathways leading to bilin (HemF, HemH and Ho1) and carotenoid (Pys and CruE) biosynthesis showed upregulation which further supports elevated need for protection against ROS in the excess of NdbA under LAHG conditions.

NdbA plays a role in expression and functionality of the photosynthetic machinery under LAHG conditions

Synechocystis cells grown under LAHG conditions develop only rudimentary and poorly organized thylakoids (Barthel et al. 2013, Plohnke et al. 2015) (**Fig. 4B**). However, the excess of NdbA in the Δ*ndbA::ndbA* strain, as compared to WT, nearly doubled the TM content under LAHG condition, inspected from the TEM images (**Fig. 4C**). The WT *Synechocystis* harbored 4–6 visible thylakoid sacks per cell, whereas the NdbA

overexpression strain, Δ*ndbA*::*ndbA*, demonstrated 8–10 thylakoid sacks in the cell image.

No effective PSII yield, Y(II), was detected from the LAHG grown WT and Δ*ndbA* (**Fig. 7C**), being in accordance with earlier observation that although both PSII and PSI accumulate in thylakoids under LAHG conditions, the PSII complexes are fully inactive (Barthel et al. 2013). Interestingly, the Δ*ndbA*::*ndbA* strain retained small but distinct effective PSII yield, Y(II), under LAHG conditions (**Fig. 7C**) together with elevated amounts of PSII subunits and several PSII assembly factors compared to WT (**Table 1**). In addition, elevated expression of CurT protein was detected in the Δ*ndbA*::*ndbA* overexpression strain under LAHG (**Table 1**), which corresponds to increased number of thylakoids in the cell. In *Synechocystis*, CurT is responsible for shaping the thylakoids and is required for generation of biogenesis centers where PSII complex components are translated and assembled (Heinz et al. 2016). This is in agreement with increased amount of PSII subunits and assembly factors (**Table 1**) as well as its small but detectable function (**Fig. 7C**) in the Δ*ndbA*::*ndbA* strain under LAHG conditions in comparison to WT.

Moreover, proteins whose expression under LAHG conditions most strikingly responded to the quantity of the NdbA protein in the TM included specific PSII regulatory proteins (**Table 1**). First, they comprised proteins that mediate NPQ in cyanobacteria (Wilson et al. 2006, Wilson et al. 2007, Boulay et al. 2010, Kirilovsky and Kerfeld 2013). OCP, which dissipates excess excitation energy captured by PBS as heat, was downregulated in Δ*ndbA*::*ndbA* (**Table 1**) but the amount of FRP, required for inactivation of OCP, showed distinct upregulation in Δ*ndbA*::*ndbA* and downregulation in Δ*ndbA* as compared to WT (**Table 1**). It was earlier demonstrated that the alterations in the amounts of both OCP and FRP (high OCP to FRP ratio) could be applied as photoprotective mechanism in cyanobacterial cells (Kirilovsky 2015). Second, the expression of the Flv2 and Flv4 proteins, which function in photoprotection of PSII (Zhang et al. 2009, Zhang et al. 2012, Bersanini et al. 2014), was attenuated in Δ*ndbA*::*ndbA* but was elevated in Δ*ndbA* as compared to WT (**Table 1**). Thus, the distinct regulation of the expression of the PSII photoprotective proteins in the NdbA mutant strains (**Table 1**) correlates not only with the amount of the NdbA protein in the TM (**Figs. 1B, 6**) but also with the effective PSII yield Y(II) under LAHG conditions (**Fig. 7C**). These findings indicate that in the excess of NdbA and under LAHG conditions, *Synechocystis* cells strive for enhancing electron flow through PSII further to the photosynthetic electron transport chain even though the PSII activity remains extremely low.

Unlike PSII, PSI was found partly functional under LAHG in *Synechocystis* (**Fig. 7D**), as also observed earlier (Barthel et al. 2013). There was, however, no significant difference in the effective PSI yield, Y(I), between WT and the two NdbA mutants (**Fig. 7D**), due to the fact that there was only minor electron input originating from PSII in all the studied strains under LAHG conditions (**Fig. 7C**). Despite this, the intracellular NdbA amount in TM had a distinct effect on the maximum amount of photo-oxidizable P700, P_m, (**Table 2**), demonstrating that NdbA is required to maintain functional PSI under LAHG conditions. Increased P_m value in the NdbA overexpression strain Δ*ndbA*::*ndbA* under LAHG conditions is also in line with elevated expression of Chl biosynthesis proteins under the same conditions. It has been demonstrated that de novo synthesis of Chl is a rate limiting factor for the translation of the PSI core subunits, and thus, the maintenance of PSI functionality is likely controlled via the regulation of Chl biosynthesis (Eichacker et al. 1996). In addition, observed upregulation of the main iron transporter FutABC (Katoh et al. 2001, Kranzler et al. 2014) in Δ*ndbA*::*ndbA* (**Table 1**) is in accordance with the maintenance of PSI because the biogenesis of functional PSI requires most iron among all photosynthetic protein complexes. All these results support the increased functional capacity of PSI under LAHG when NdbA is overexpressed.

In addition to PSII and PSI activities, the NdbA amount in TM under LAHG conditions correlates with the protein amount of major components of the linear electron transfer chain: the Cyt b_6f complex together with soluble electron carriers cytochrome c_6 (Cyt c_6) and several ferredoxins were at elevated level in the Δ*ndbA*::*ndbA* compared to WT (**Table 1**). Increased abundance of Cyt c_6, the alternative electron transfer component to plastocyanin (PC), implies copper deficiency. In parallel, two systems regulating copper homeostasis in the cell, CopBAC and CopMRS, were downregulated in Δ*ndbA*::*ndbA* (**Table 1**), whereas another protein SynAtx1, involved in protection of *Synechocystis* against free cupric ions in cytoplasm, was upregulated in Δ*ndbA*::*ndbA*. SynAtx1 is the copper metallochaperone and interacts with CtaA or PacS to ensure transport of redundant copper ions to the cytosol or lumen, respectively (Giner-Lamia et al. 2012, Giner-Lamia et al. 2014). It is thus highly conceivable that copper availability is a limiting factor for PC synthesis in the excess of NdbA under LAHG conditions, and is thus complemented with Cyt c_6, which is a typical response in cyanobacteria and green algae under copper deficiency (Zhang et al. 1992).

Taken together, it is relevant to conclude that NdbA is required for the adjustment of redundant expression and functionality of the photosynthetic machinery under LAHG conditions. The requirement of some photosynthetic activity upon a short daily exposure of cells to light is apparently important to coordinate the metabolic functions of the cells under LAHG conditions.

NdbA is involved in regulation of C_i uptake under LAHG conditions

Another group of proteins whose expression under LAHG conditions follows the amount of the NdbA protein in TM (**Figs. 3B, 6**) comprises the proteins involved in CCM of *Synechocystis* (**Table 1**). Clearly, the overexpression of NdbA causes downregulation of the C_i uptake protein complexes, like BCT1, SbtA, SbtB and NDH-1$_3$ under LAHG conditions whereas the deletion of NdbA in the TM of Δ*ndbA* causes slight increase in C-acquisition components as compared to WT (**Table 1**).

CO_2 fixation is not expected to be required to support the growth of Synechocystis under LAHG conditions due to extensive utilization of glucose (Plohnke et al. 2015). Indeed, the depletion of the cell from energy-consuming C_i acquisition mechanisms, as occurs in $\Delta ndbA::ndbA$ that overexpresses NdbA and to the lesser extent in WT as compared to the $\Delta ndbA$, is likely to provide possibilities for investing the available energy in more crucial metabolism than CCM under LAHG conditions.

Hypothetical regulatory function of NdbA under LAHG

NDH-2s in Synechocystis have been demonstrated to oxidize NADH and transfer electrons to quinone acceptors (Howitt et al. 1999). However, only cells grown under PA and mixotrophic conditions were previously studied and no intracellular location or specific function was addressed for NdbA. Our results provide compelling evidence that NdbA, shown here to be an intrinsic protein in the TM (**Fig. 1**), is an important component for the maintenance of functional PSII and PSI under LAHG conditions (**Fig. 7C**, **Table 2**). This was particularly apparent in the NdbA overexpression strain $\Delta ndbA::ndbA$ concerning PSI, which is likely to result mainly from improved regulation (e.g. the Fe-S centers; (Tiwari et al. 2016), as such drastic differences were not observed in the amount of PSI subunits (**Table 1**). Contribution of NdbA to PSI functionality is particularly demonstrated by the high P_m value (**Table 2**), describing the maximal content of oxidizable P700, when NdbA is produced in excess under LAHG conditions. However, improved function of photosystems as such does not give any growth benefit (**Fig. 2C**) and thus the importance of the short daily illumination period for successful LAHG growth most likely relies on supporting the regulatory functions.

As the growth under LAHG conditions is maintained by sugar catabolism (Plohnke et al. 2015) that produces NADH in high amounts as a substrate for NdbA, the deletion of NdbA is expected to reduce and NdbA overexpression to enhance the electron supply to TM located electron transfer chain. The importance of the functionality of photosynthetic electron transfer upon the short daily illumination periods might become important for production of proper signaling components required for optimal gene regulation at transcriptional level. Changes in the redox state of various components of the electron transport chain, production of distinct reactive oxygen species by the photosystems as well as various metabolites activated on reducing side of PSI are likely to relay information for transcriptional regulation of genes in photosynthetic cyanobacteria (Hihara et al. 2001, Wilde and Hihara 2016). NdbA, an intrinsic thylakoid protein with redox activity, is likely to be involved in such signaling processes to modulate the gene expression of Synechocystis cells at protein level (**Table 1**). However, such a function does not provide an unambiguous explanation for the function of NdbA in promoting growth under LAHG conditions, due to the fact that the overexpression of NdbA showed no further acceleration of growth (**Fig. 2**).

Considering the physiological background for the retardation of growth under LAHG conditions, it is most relevant to focus on proteins whose expression was hampered in the absence of NdbA. The most striking and specific consequence of the deletion of NdbA under LAHG conditions, in comparison to WT Synechocystis cells, was the reduced expression of several proteins involved in iron utilization (**Table 1**) and in the functionality of the iron–sulfur cluster containing PSI (**Table 2**). On the contrary, the shift of WT cells from PA to LAHG conditions induced the expression of the NdbA protein, which could hardly be detected by MS approaches under PA conditions. In addition to NdbA, only a few proteins showed significantly higher expression in WT than in $\Delta ndbA$ under LAHG conditions, with nearly all of them being related to Fe homeostasis. This suggests that under LAHG conditions the inabilities in iron metabolism are likely responsible for the major physiological hurdles resulting in retarded growth in the absence of NdbA.

Materials and Methods

Strains and culture conditions

A glucose-tolerant Synechocystis sp. PCC 6803 (WT) was used as the reference strain. The $\Delta ndbA$ mutant was obtained by disruption of ndbA gene by erythromycin resistance cassette and the $\Delta ndbA::ndbA$ strain by inserting functional ndbA gene to the $\Delta ndbA$ mutant (for more details see Mutagenesis section). Pre-experimental cultures were grown in BG11 medium buffered with 20 mM HEPES-NaOH (pH 7.5) under continuous white light of 50 µmol photons m^{-2} s^{-1} at 30°C, under air enriched with 3% CO_2 with agitation of 150 rpm. Experimental cultures were grown in BG11 medium buffered with 20 mM HEPES-NaOH (pH 7.5) under ambient CO_2 concentration and continuous illumination of 50 µmol photons m^{-2} s^{-1} (photoautotrophic growth = PA), under mixotrophic growth conditions (MIXO), where in addition to continuous illumination of 50 µmol photons m^{-2} s^{-1} also 10 mM glucose was added to BG11 medium, while upon LAHG conditions the illumination was restricted to 10 min per 24 h and 10 mM glucose was provided in the growth medium. All experimental cultures were grown in growth chambers with cool-white LEDs (AlgaeTron AG130 by PSI Instruments, Czech) at 30°C with agitation of 150 rpm without antibiotics. OD$_{750}$ was measured using Lambda 25 UV/VIS spectrometer (PerkinElmer). For physiological, structural and activity measurements, as well as for protein extraction, cells were harvested from pre-experimental phase, inoculated to OD$_{750}$ = 0.1 and shifted to experimental conditions for 4 d. For activity measurements, the cells were harvested and resuspended in fresh BG11 medium at the desired Chl concentration. To monitor the growth, cells were inoculated to fresh BG11 medium at OD$_{750}$ = 0.1 in the beginning of the experiment.

Mutagenesis

The ndbA gene (slr0851) interrupted with erythromycin resistance cassette and the gene flanking regions were amplified by PCR from the $\Delta ndbA$ mutant constructed by Howitt et al. (1999) using the following primers: forward primer 5′-TATTGCCGGAGCCTTAGTGAG-3′ and reverse primer 5′- GCCAAGCTTCTACCCTCCTC -3′. The resulting PCR product was transformed into WT cells using a protocol described by Eaton-Rye (2011). Transformants were segregated by gradually raising the concentration of erythromycin (from 5 µg ml^{-1} to 25 µg ml^{-1}). Complete segregation of the mutation was confirmed by PCR (Supplementary Fig. S1).

The $\Delta ndbA::ndbA$ strain was constructed by using the same protocol as described above for transforming the $\Delta ndbA$ mutant with a construct containing the ndbA gene under psbAII promoter with adjacent kanamycin resistance cassette as a selective marker. The construct was amplified with primers: forward primer 5′-CATGCGGGGCCCGGAACAGGACCAAGCCTTGATG-3′

and reverse primer 5′-CATGCGGAGCTCCAATCCACTGATTTTGTTCAGCTA-3′ and inserted to the chromosomal *psbAI* site by homologous recombination. Transformants were segregated by gradually raising the concentration of kanamycin (from 10 μg ml^{-1} to 50 μg ml^{-1}). The correct insertion and the segregation were verified by PCR analysis using primers described above (Supplementary Fig. S1B).

Room temperature whole cell absorption spectra

Room temperature whole cell absorption spectra were measured using Olis 17 UV/VIS/NIR Spectrophotometer (On-Line Instrument Systems, Inc.). Fry's correction was applied to correct the raw spectra. The OD$_{750}$ of cells was adjusted to 0.3 before measurement.

Fluorescence measurements and P700 absorbance

The Chl fluorescence from intact cells was recorded with a pulse amplitude modulated fluorometer Dual-PAM-100 (Walz, Germany). Before measurements, cell suspensions at a Chl concentration of 15 μg ml^{-1} were dark-acclimated for 10 min. Saturating pulses of 5,000 μmol photons m^{-2} s^{-1} (300 ms) and a strong far-red light (720 nm, 75 W m^{-2}) were applied to samples when required. 50 μmol photons m^{-2} s^{-1} was applied as actinic light. The effective yield of PS II, Y(II), was calculated as (F$_{m'}$ − F$_s$)/F$_{m'}$. The P700 signal was recorded simultaneously with fluorescence. The maximal change in the P700 signal (P$_m$) upon transformation of P700 from fully reduced to fully oxidized state was achieved by applying a saturation pulse on the FR background illumination. The effective yield of PSI, Y(I), was calculated as (P$_{m'}$ − P)/P$_m$.

Western blotting; protein isolation, electrophoresis and immunodetection

Total protein extracts of *Synechocystis* cells were isolated as described by Zhang et al. (2009). Proteins were separated by 12% (w/v) SDS-PAGE containing 6 M urea, transferred to a PVDF membrane (Immobilon-P, Millipore) and analyzed with the protein-specific antibodies. The membrane fractions to confirm the localization of NdbA were prepared as described by Zhang et al. (2004). A specific antibody against NdbA was raised by Agrisera.

Transmission electron microscopy

TEM-analysis was performed in the Laboratory of Electron Microscopy (University of Turku). Samples were prefixed with 5% glutaraldehyde in a 0.16 M s-collidin buffer (pH 7.4) and postfixed with 2% OsO$_4$ + 3% K-ferrocyanide. After this samples were dehydrated, embedded and cut to thin sections (70 nm). These were stained with 1% uranyl acetate and 0.3% lead citrate. A JEM-1400 Plus Transmission Electron Microscope (JEOL) was used in the analysis.

Mass spectrometry—data dependent acquisition (DDA)

For liquid chromatography-tandem mass spectrometry (LC-ESI-MS/MS) analysis the total proteins were isolated and digested as described by Vuorijoki et al. (2016) with one modification: ammonium bicarbonate buffer NH$_4$HCO$_3$ was replaced by Tris-HCl buffer (pH 8.0) of equal molarity for extraction and digestion steps.

The LC-ESI-MS/MS analyses were performed on a nanoflow HPLC system (Easy-nLC1200, Thermo Fisher Scientific) coupled to the Q Exactive HF mass spectrometer (Thermo Fisher Scientific) equipped with a nano-electrospray ionization source. The four biological replicates from each condition were injected on an analytical C18 column (75 μm × 40 cm, ReproSil-Pur 1.9 μm 120 Å C18-AQ, Dr. Maisch HPLC GmbH, Ammerbuch-Entringen, Germany). The mobile phase consisted of water with 0.1% formic acid (solvent A) or acetonitrile/water [80:20 (v/v)] with 0.1% formic acid (solvent B). Peptides were separated by a two-step 110 min gradient from 5% to 26% B in 70 min followed by 26% to 49% B increase in 30 min.

MS data were acquired automatically by using Thermo Xcalibur 3.1 software (Thermo Fisher Scientific). A data dependent acquisition method consisted of an Orbitrap MS survey scan of mass range 300–1,800 *m/z* followed by HCD fragmentation for 12 most intense peptide ions. The spectra were registered with a resolution of 120,000 and 15,000 (at *m/z* 200) for full scan and for fragment ions, respectively, and normalized collision energy of 27%. The automatic gain control was set to a maximum fill time of 100 ms and 250 ms to obtain maximum number of 3e6 and 1e5 ions for MS and MS/MS scans, respectively.

Data files were searched for protein identification against *Synechocystis* database retrieved from Cyanobase (Kaneko et al. 1996) (3672 entries, October 23, 2012) using Proteome Discoverer 2.2 software (Thermo Fisher Scientific) connected to an in-house server running the Mascot 2.6.1 (Perkins et al. 1999) algorithm (Matrix Science). The precursor value was restricted to monoisotopic with a mass tolerance of ±4 ppm and fragment ion mass tolerance of ±0.02 Da. Two missed cleavages were allowed and decoy searches were performed. For the validation of the spectrum identifications, we used a Percolator algorithm (Käll et al. 2007) with relaxed false discovery rate of 0.05. The mass spectrometry proteomics data have been deposited to the ProteomeXchange Consortium (Deutsch et al. 2017) via the PRIDE partner repository with dataset identifier PXD011671 and 10.6019/PXD011671 (Vizcaíno et al. 2016). Quantitative analysis was done in Progenesis software with global normalization and using relative quantification of proteins with at least two peptides with no conflicts per protein.

Author contributions

The concept of the study - T.H.&E.M.A, acquisition, analysis and data interpretation - T.H., D.M.P. & E.M.A, writing of the manuscript T.H., D.M.P. & E.M.A.

References

Barthel, S., Bernát, G., Seidel, T., Rupprecht, E., Kahmann, U. and Schneider, D. (2013) Thylakoid membrane maturation and PSII activation are linked in greening *Synechocystis* sp. PCC 6803 cells. *Plant Physiol.* 163: 1037–1046.

Battchikova, N., Eisenhut, M. and Aro, E.M. (2011) Cyanobacterial NDH-1 complexes: Novel insights and remaining puzzles. *Biochim. Biophys. Acta* 1807: 935–944.

Bersanini, L., Battchikova, N., Jokel, M., Rehman, A., Vass, I. and Allahverdiyeva, Y. (2014) Flavodiiron protein Flv2/Flv4-related photoprotective mechanism dissipates excitation pressure of PSII in cooperation with phycobilisomes in Cyanobacteria. *Plant Physiol.* 164: 805–818.

Boulay, C., Wilson, A., D'Haene, S. and Kirilovsky, D. (2010) Identification of a protein required for recovery of full antenna capacity in OCP-related photoprotective mechanism in cyanobacteria. *Proc. Natl. Acad. Sci. USA* 107: 11620–11625.

Deutsch, E.W., Csordas, A., Sun, Z., Jarnuczak, A., Perez-Riverol, Y., Ternent, T., et al. (2017) The ProteomeXchange consortium in 2017: supporting the cultural change in proteomics public data deposition. *Nucleic Acids Res.* 45: D1100–D1106.

Eaton-Rye, J.J. (2011) Construction of gene interruptions and gene deletions in the cyanobacterium Synechocystis sp. strain PCC 6803. Methods Mol Biol 684: 295–312.

Eichacker, L.A., Helfrich, M., Rüdiger, W. and Müller, B. (1996) Stabilization of chlorophyll a-binding apoproteins P700, CP47, CP43, D2, and D1 by chlorophyll a or Zn-pheophytin a. J. Biol. Chem. 271: 32174–32179.

Fang, L., Ge, H., Huang, X., Liu, Y., Lu, M., Wang, J., et al. (2017) Trophic mode-dependent proteomic analysis reveals functional significance of light-independent chlorophyll synthesis in Synechocystis sp. PCC 6803. Mol. Plant 10: 73–85.

Fatihi, A., Latimer, S., Schmollinger, S., Block, A., Dussault, P.H., Vermaas, W.F.J., et al. (2015) A dedicated type II NADPH dehydrogenase performs the penultimate step in the biosynthesis of vitamin K1 in Synechocystis and Arabidopsis. Plant Cell. 27: 1730–1741.

Fujita, Y. (1996) Protochlorophyllide reduction: a key step in the greening of plants. Plant Cell Physiol. 37: 411–421.

Giner-Lamia, J., López-Maury, L. and Florencio, F.J. (2014) Global transcriptional profiles of the copper responses in the cyanobacterium Synechocystis sp. PCC 6803. PLoS One 9: e108912.

Giner-Lamia, J., Lopez-Maury, L., Reyes, J.C. and Florencio, F.J. (2012) The CopRS two-component system is responsible for resistance to copper in the cyanobacterium Synechocystis sp. PCC 6803. Plant Physiol. 159: 1806–1818.

Heinz, S., Rast, A., Shao, L., Gutu, A., Gügel, I.L., Heyno, E., et al. (2016) Thylakoid membrane architecture in Synechocystis depends on CurT, a homolog of the granal CURVATURE THYLAKOID1 proteins. Plant Cell 28: 2238–2260.

Hihara, Y., Kamei, A., Kanehisa, M., Kaplan, A. and Ikeuchi, M. (2001) DNA microarray analysis of cyanobacterial gene expression during acclimation to high light. Plant Cell 13: 793–806.

Howitt, C.A., Udall, P.K. and Vermaas, W.F. (1999) Type 2 NADH dehydrogenases in the cyanobacterium Synechocystis sp. strain PCC 6803 are involved in regulation rather than respiration. J. Bacteriol. 181: 3994–4003.

Huokko, T., Muth-Pawlak, D., Battchikova, N., Allahverdiyeva, Y. and Aro, E.-M. (2017) Role of type 2 NAD(P)H dehydrogenase NdbC in redox regulation of carbon allocation in Synechocystis. Plant Physiol. 174: 1863–1880.

Kada, S., Koike, H., Satoh, K., Hase, T. and Fujita, Y. (2003) Arrest of chlorophyll synthesis and differential decrease of photosystems I and II in a cyanobacterial mutant lacking light-independent protochlorophyllide reductase. Plant Mol. Biol. 51: 225–235.

Käll, L., Canterbury, J.D., Weston, J., Noble, W.S. and MacCoss, M.J. (2007) Semi-supervised learning for peptide identification from shotgun proteomics datasets. Nat. Methods 4: 923–925.

Kaneko, T., Sato, S., Kotani, H., Tanaka, A., Asamizu, E., Nakamura, Y., et al. (1996) Sequence analysis of the genome of the unicellular cyanobacterium Synechocystis sp. strain PCC6803. II. Sequence determination of the entire genome and assignment of potential protein-coding regions. DNA Res. 3: 109–136.

Katoh, H., Hagino, N., Grossman, A.R. and Ogawa, T. (2001) Genes essential to iron transport in the cyanobacterium Synechocystis sp. strain PCC 6803. J. Bacteriol. 183: 2779–2784.

Kirilovsky, D. (2015) Modulating energy arriving at photochemical reaction centers: orange carotenoid protein-related photoprotection and state transitions. Photosynth. Res. 126: 3–17.

Kirilovsky, D. and Kerfeld, C.A. (2013) The Orange Carotenoid Protein: a blue-green light photoactive protein. Photochem. Photobiol. Sci. 12: 1135.

Knowles, V.L. and Plaxton, W.C. (2003) From genome to enzyme: analysis of key glycolytic and oxidative pentose-phosphate pathway enzymes in the cyanobacterium Synechocystis sp. PCC 6803. Plant Cell Physiol. 44: 758–763.

Kranzler, C., Lis, H., Finkel, O.M., Schmetterer, G., Shaked, Y. and Keren, N. (2014) Coordinated transporter activity shapes high-affinity iron acquisition in cyanobacteria. ISME J. 8: 409–417.

Kruger, N.J. and Von Schaewen, A. (2003) The oxidative pentose phosphate pathway: structure and organisation. Curr. Opin. Plant Biol. 6: 236–246.

Kurian, D., Jansèn, T. and Mäenpää, P. (2006) Proteomic analysis of heterotrophy in Synechocystis sp. PCC 6803. Proteomics 6: 1483–1494.

Latifi, A., Ruiz, M. and Zhang, C.C. (2009) Oxidative stress in cyanobacteria. FEMS Microbiol. Rev. 33: 258–278.

Marreiros, B.C., Sena, F.V., Sousa, F.M., Batista, A.P. and Pereira, M.M. (2016) Type II NADH: quinone oxidoreductase family: phylogenetic distribution, structural diversity and evolutionary divergences. Environ. Microbiol. 18: 4697–4709.

Marreiros, B.C., Sena, F.V., Sousa, F.M., Oliveira, A.S.F., Soares, C.M., Batista, A.P., et al. (2017) Structural and functional insights into the catalytic mechanism of the type II NADH: quinone oxidoreductase family. Sci. Rep. 7: 1–13.

Melo, A.M.P., Bandeiras, T.M. and Teixeira, M. (2004) New insights into type II NAD(P)H: quinone oxidoreductases new insights into type II NAD(P)H: quinone oxidoreductases. Microbiol. Mol. Biol. Rev. 68: 603–616.

Mohamed, H.E. and Vermaas, W.F.J. (2006) Sll0254 (CrtL(diox)) is a bifunctional lycopene cyclase/dioxygenase in cyanobacteria producing myxoxanthophyll. J. Bacteriol. 188: 3337–3344.

Mullineaux, C.W. (2014) Co-existence of photosynthetic and respiratory activities in cyanobacterial thylakoid membranes. Biochim. Biophys. Acta 1837: 503–511.

Omata, T., Price, G.D., Badger, M.R., Okamura, M., Gohta, S. and Ogawa, T. (1999) Identification of an ATP-binding cassette transporter involved in bicarbonate uptake in the cyanobacterium Synechococcus sp. strain PCC 7942. Proc. Natl. Acad. Sci. USA 96: 13571–13576.

Osanai, T., Kanesaki, Y., Nakano, T., Takahashi, H., Asayama, M., Shirai, M., et al. (2005) Positive regulation of sugar catabolic pathways in the cyanobacterium Synechocystis sp. PCC 6803 by the group 2 sigma factor sigE. J. Biol. Chem. 280: 30653–30659.

Peltier, G., Aro, E.-M. and Shikanai, T. (2016) NDH-1 and NDH-2 plastoquinone reductases in oxygenic photosynthesis. Annu. Rev. Plant Biol. 67: 55–80.

Perkins, D.N., Pappin, D.J.C., Creasy, D.M. and Cottrell, J.S. (1999) Probability-based protein identification by searching sequence databases using mass spectrometry data. Electrophoresis 20: 3551–3567.

Plohnke, N., Seidel, T., Kahmann, U., Rögner, M., Schneider, D. and Rexroth, S. (2015) The proteome and lipidome of Synechocystis sp. PCC 6803 cells grown under light-activated heterotrophic conditions. Mol. Cell. Proteomics 14: 572–584.

Shen, G., Balasubramanian, R., Wang, T., Wu, Y., Hoffart, L.M., Krebs, C., et al. (2007) SufR coordinates two [4Fe-4S]2+, 1+ clusters and functions as a transcriptional repressor of the sufBCDS operon and an autoregulator of sufR in cyanobacteria. J. Biol. Chem. 282: 31909–31919.

Shibata, M., Katoh, H., Sonoda, M., Ohkawa, H., Shimoyama, M., Fukuzawa, H., et al. (2002) Genes essential to sodium-dependent bicarbonate transport in cyanobacteria: function and phylogenetic analysis. J. Biol. Chem. 277: 18658–18664.

Shpilyov, A.V., Zinchenko, V.V., Grimm, B. and Lokstein, H. (2013) Chlorophyll a phytylation is required for the stability of photosystems I and II in the cyanobacterium Synechocystis sp. PCC 6803. Plant J. 73: 336–346.

Strand, D.D., Fisher, N. and Kramer, D.M. (2017) The higher plant plastid NAD(P)H dehydrogenase-like complex (NDH) is a high efficiency proton pump that increases ATP production by cyclic electron flow. J. Biol. Chem. 292: 11850–11860.

Tiwari, A., Mamedov, F., Grieco, M., Suorsa, M., Jajoo, A., Styring, S., et al. (2016) Photodamage of iron-sulphur clusters in photosystem I induces non-photochemical energy dissipation. *Nat. Plants* 2.

Vermaas, W. (2001) *Photosynthesis and Respiration in Cyanobacteria. In* eLS, John Wiley & Sons, London, UK.

Vizcaíno, J.A., Csordas, A., del-Toro, N., Dianes, J.A., Griss, J., Lavidas, I., et al. (2016) 2016 update of the PRIDE database and its related tools. *Nucleic Acids Res.* 44: D447–D456.

Vuorijoki, L., Isojärvi, J., Kallio, P., Kouvonen, P., Aro, E.M., Corthals, G.L., et al. (2016) Development of a quantitative SRM-based proteomics method to study iron metabolism of *Synechocystis* sp. PCC 6803. *J. Proteome Res.* 15: 266–279.

Wan, N., DeLorenzo, D.M., He, L., You, L., Immethun, C.M., Wang, G., et al. (2017) Cyanobacterial carbon metabolism: fluxome plasticity and oxygen dependence. *Biotechnol. Bioeng.* 114: 1593–1602.

Wierenga, R.K., Terpstra, P. and Hol, W.G.J. (1986) Prediction of the occurrence of the ADP-binding βαβ-fold in proteins, using an amino acid sequence fingerprint. *J. Mol. Biol.* 187: 101–107.

Wilde, A. and Hihara, Y. (2016) Transcriptional and posttranscriptional regulation of cyanobacterial photosynthesis. *Biochim. Biophys. Acta* 1857: 296–308.

Wilson, A., Ajlani, G., Verbavatz, J.-M., Vass, I., Kerfeld, C.A. and Kirilovsky, D. (2006) A soluble carotenoid protein involved in phycobilisome-related energy dissipation in cyanobacteria. *Plant Cell* 18: 992–1007.

Wilson, A., Boulay, C., Wilde, A., Kerfeld, C.A. and Kirilovsky, D. (2007) Light-induced energy dissipation in iron-starved cyanobacteria: roles of OCP and IsiA proteins. *Plant Cell* 19: 656–672.

Yagi, T. (1991) Bacterial NADH-quinone oxidoreductases. *J. Bioenerg. Biomembr.* 23: 211–225.

Yang, C., Hua, Q. and Shimizu, K. (2002) Metabolic flux analysis in *Synechocystis* using isotope distribution from 13C-labeled glucose. *Metab. Eng.* 4: 202–216.

Zhang, L., McSpadden, B., Pakrasi, H.B. and Whitmarsh, J. (1992) Copper-mediated regulation of cytochrome c553 and plastocyanin in the cyanobacterium *Synechocystis* 6803. *J. Biol. Chem.* 267: 19054–19059.

Zhang, P., Allahverdiyeva, Y., Eisenhut, M. and Aro, E.M. (2009) Flavodiiron proteins in oxygenic photosynthetic organisms: photoprotection of photosystem II by Flv2 and Flv4 in *Synechocystis* sp. PCC 6803. *PLoS One* 4: e5331.

Zhang, P., Battchikova, N., Jansen, T., Appel, J., Ogawa, T. and Aro, E. (2004) Expression and functional roles of the two distinct NDH-1 complexes and the carbon acquisition complex NdhD3/NdhF3/CupA/Sll1735 in *Synechocystis* sp. PCC 6803. *Plant Cell* 16: 3326–3340.

Zhang, P., Eisenhut, M., Brandt, A.-M., Carmel, D., Silen, H.M., Vass, I., et al. (2012) Operon flv4-flv2 provides cyanobacterial photosystem II with flexibility of electron transfer. *Plant Cell* 24: 1952–1971.